

SPECT image reconstruction using compound prior models ^{*}

A. E. López†, R. Molina‡, A. K. Katsaggelos§, J. Mateos‡

†Universidad de Granada. Departamento de Lenguajes y Sistemas Informáticos.
18071 Granada, Spain. alopez@goliat.ugr.es

‡Universidad de Granada. Departamento de Ciencias de la Computación e I.A.
18071 Granada, Spain. {rms,jmd}@decsai.ugr.es

§Northwestern University. Department of Electrical and Computer Engineering.
Evanston, Illinois 60208-3118, aggk@ece.nwu.edu

Abstract

SPECT (Single Photon Emission Computed Tomography) is used in nuclear medicine to determine the distribution of a radioactive isotope within a patient from tomographic view or projection data. These projections are severely degraded due to the presence of noise and several physical factors like attenuation and scattering. We use, within the Bayesian framework, Compound Gauss Markov Random Fields (CGMRF) as models to reconstruct such images. In order to find the Maximum a Posteriori (MAP) estimate we propose a new iterative method, which is stochastic for the line process and deterministic for the reconstruction. The proposed method is tested and compared with other existing methods on real and synthetic images.

Keywords: SPECT imaging, line process, deterministic image restoration.

1 Introduction

SPECT images are observation data acquired by a gamma-camera following an orbit around the patient's body, at regularly spaced angles. A reconstructed image is the discrete representation of a slice or cross section of the isotope distribution within the patient, transversal to the gamma-camera rotation axis.

Bayesian reconstruction methods have been extensively used to reconstruct medical images since they can improve the reconstructions with respect to the classical non statistical methods, such as FBP (Filtered Back Projection)[1].

In the Bayesian paradigm, the reconstructed image \hat{X} is usually selected as

$$\hat{X} = \arg \max_X P(X|Y) = \arg \max_X P(Y|X)P(X), \quad (1)$$

^{*} This work has been partially supported by the "CICYT" under contracts TIC97-0989 and TIC2000-1275

where $P(X)$ is a prior distribution incorporating information about the expected structure in the image X , and $P(Y|X)$ models the degradation process of projections Y from the pixel intensities of the emission source (patient).

The rest of the paper is organized as follows. In section 2 we define the degradation and image models. Then, in section 3 we propose a new method for finding the MAP estimate. The application of this method to synthetic and real images is described in section 4. Finally, the section 5 concludes the paper.

2 Degradation and image models

The degradation model for emission tomography can be specified as a product of independent Poisson distributions

$$P(y|x) = \prod_{s=1}^M \frac{(\sum_{i=1}^N A_{s,i}x_i)^{y_s} \exp\{-\sum_{t=1}^N A_{s,t}x_t\}}{y_s!}, \quad (2)$$

M is the number of detectors, N is the number of pixels and A is the system matrix. $A_{s,i}$ is the probability that an emitted photon from pixel i reaches detector s .

The prior model we use is a CGMRF model. This model provides us with a means to control changes in the image using a hidden random field. A CGMRF model has two levels, an upper level which is the image to restore and the lower or hidden level that it is an underlying random field, called the line process, to govern the transition between the sub-models. The use of a line process, was introduced in [2] for the discrete case. Extensions to the continuous case were presented in [3].

The CGMRF model to be used is introduced from a simpler one, the Conditional Auto-Regression (CAR) model[4]. This prior model is defined by

$$P(X) \propto \exp\{-\frac{1}{2}\alpha X^t(I - \phi C)X\} \quad (3)$$

where, for an 8-point neighborhood system, $C_{i,j} = 2(0.5\sqrt{2} + 1)^{-1}$ for nearest neighbor pixels i and j , $C_{i,j} = 2(\sqrt{2} + 1)^{-1}$ for diagonal neighbors and zero otherwise, α is a scaling parameter, and $|\phi| \leq 1/8$.

If we assume a "toroidal edge correction", we introduce the line process by rewriting the Eq. (3) as

$$\begin{aligned} -\log P(X) \propto & \frac{\alpha\phi}{2} \left(\sum_i C_{i,i:1}(x_i - x_{i:1})^2(1 - l_{[i,i:1]}) + \sum_i C_{i,i:2}(x_i - x_{i:2})^2(1 - l_{[i,i:2]}) \right) \\ & + \frac{\alpha\phi}{2} \left(\sum_i C_{i,i:5}(x_i - x_{i:5})^2(1 - l_{[i,i:5]}) + \sum_i C_{i,i:6}(x_i - x_{i:6})^2(1 - l_{[i,i:6]}) \right) \end{aligned}$$

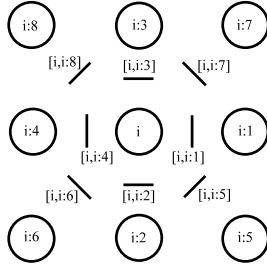


Figure 1: Image and line sites

$$+ \frac{\alpha}{2} \sum_i \left[\beta l_{[i,i:1]} + \beta l_{[i,i:2]} + \beta l_{[i,i:5]} + \beta l_{[i,i:6]} \right] + \frac{\alpha}{2} \sum_i (1 - 8\phi) x_i^2, \quad (4)$$

where $i:1, i:2, \dots, i:8$ are the eight pixels around pixel i (see figure 1). The element $l([i, j])$ takes the value zero if pixels i and j are not separated by an active line and one otherwise. The parameter β is a scalar weight, which adjusts the introduction of the active line elements. For β very large the prior model becomes Gaussian. The process line acts as inhibitor or activator of the relation between two neighboring pixels depending on whether or not there exists an edge.

3 MAP estimation

Let us now proceed to find \hat{X}, \hat{L} , the MAP estimates of X and L , that is

$$\hat{X}, \hat{L} = \arg \max_{X, L} P(X, L|Y). \quad (5)$$

Since $P(X, L|Y)$ is nonlinear, it is difficult to find \hat{X} and \hat{L} by conventional methods, such as simulated annealing [5]. The method we propose for estimating the original image and the line process is stochastic for the line process and deterministic for the reconstruction, as described next.

In order to estimate the line process we simulate the corresponding conditional a posteriori density function. Let us denote by $P_T(l_{[i,j]}|L_{[i,j]}, X, Y)$ the conditional a posteriori density function for the line process $l_{[i,j]}$, given X, Y and the rest of $L, L_{[i,j]} = (l_{[s,t]} : \forall [s,t] \neq [i,j])$. To simulate this density function, we have

$$P_T(l_{[i,j]} = 0|L_{[i,j]}, X, Y) \propto \exp \left[-\frac{1}{T} \frac{\alpha \phi C_{i,j}}{2} (x_i - x_j)^2 \right] \quad (6)$$

$$P_T(l_{[i,j]} = 1|L_{[i,j]}, X, Y) \propto \exp \left[-\frac{1}{T} \frac{\alpha \beta}{2} \right], \quad (7)$$

where T is the temperature.

Given an estimate of the line process, L , and the observation, Y , to estimate the image X we use a deterministic method which take into account only neighbors not separated by an active line element. Starting from the probability distribution $P(X|L, Y)$, we obtain the following iterative equation

$$x_i = \mu_i \left(\phi \sum_{j \in \mathcal{N}_i} x_j C_{i,j} (1 - l_{[i,j]}) + \phi x_i \sum_{j \in \mathcal{N}_i} C_{i,j} l_{[i,j]} \right) + (1 - \mu_i) x_i \sum_{s=1}^M \frac{y_s A_{s,i}}{\sum_{t=1}^N A_{s,t} x_t}, \quad (8)$$

with $\mu_i = x_i / (x_i + \alpha^{-1})$.

We can now use Eqs. (6), (7) and (8) in the following algorithm to find the MAP estimates of L and X :

Let $k = 1, 2, \dots$, be the sequence of iterations in which the sites (lines or pixels) are visited for updating.

1. Set $k = 0$ and assign an initial configuration denoted as X_{-1} , L_{-1} and a initial temperature $T = 1$.
2. The evolution $\hat{L}_{k-1} \rightarrow \hat{L}_k$ of the line process is simulated by the probability functions defined in Eqs. (6) and (7).
3. The evolution $\hat{X}_{k-1} \rightarrow \hat{X}_k$ of the image is obtained using \hat{X}_{k-1} in the right hand part of Eq. (8) and X_k in the left hand part of Eq. (8).
4. Set $k = k + 1$. Decrease the temperature T according to an annealing scheme [3]. Go to step 2 until $k > N$, where N is a specified integer.

4 Experimental results

We compare the results using the proposed method with the reconstruction obtained by FBP and CAR and GGMRF (Generalized Gauss Markov Random Field) [6] priors. For the last models, the scaling parameters for the reconstruction were obtained using the estimation process described in [7]. The methods were tested on the 128x128 pixels synthetic image depicted in Fig. 2(a). A circular orbit with 128 detectors and 128 angles are simulated. The corresponding sinogram is shown in Fig. 2(b). We can observe that the method with a CAR prior penalizes in excess the edges (see Fig. 2(c)), while the method with the GGMRF prior, Fig. 2(d), preserves the edges when the shape parameter is near 1 (for our experiments we used a shape parameter fixed to 1.1). The reconstruction with CGMRF, Fig. 2(e), shows an improved reconstruction. Fig. 2(f) shows the edges corresponding to Fig. 2(e). It is clear that the proposed method has captured the edges present in the

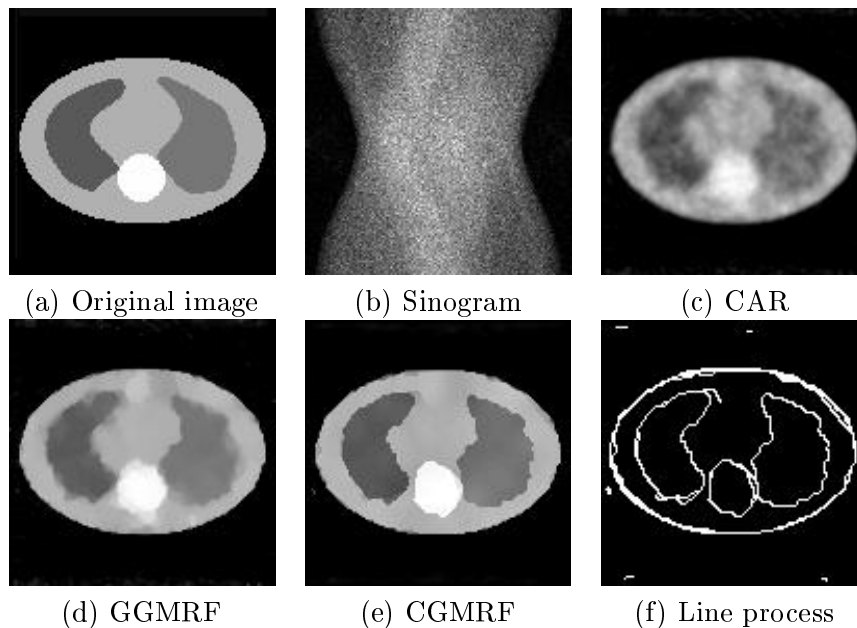


Figure 2: Results with a synthetic image.

image. We also applied our reconstruction method to real images (see Fig. 3). The detector system was a Siemens Orbiter 66601 and the collimator was a parallel hole. The gamma-camera described a circular orbit, at 5.625 degrees steps (there are 64 angles). The image corresponds to the inferior part of the liver (the right lobe and the center posterior hepatic zone, crossed there by blood vessels). The data provided by the detector system and its FBP reconstruction can be observed in Fig. 3(a) and (b), respectively. In Figs. 3(c) and 3(d) we show the reconstructions with CAR and GGMRF priors. The reconstruction with the proposed method and the corresponding line process are shown respectively in Fig. 3(e) and 3(f). The proposed method clearly increases the quality of the reconstruction since the areas with different levels of vascularization can be better distinguished.

5 Conclusions

In this paper we have presented a new method that can be used to reconstruct SPECT images. This method uses a prior model with a line process and the MAP estimation is performed by simulated annealing for the line process and a deterministic iterative scheme for the image. The experimental results show the validity of the method.

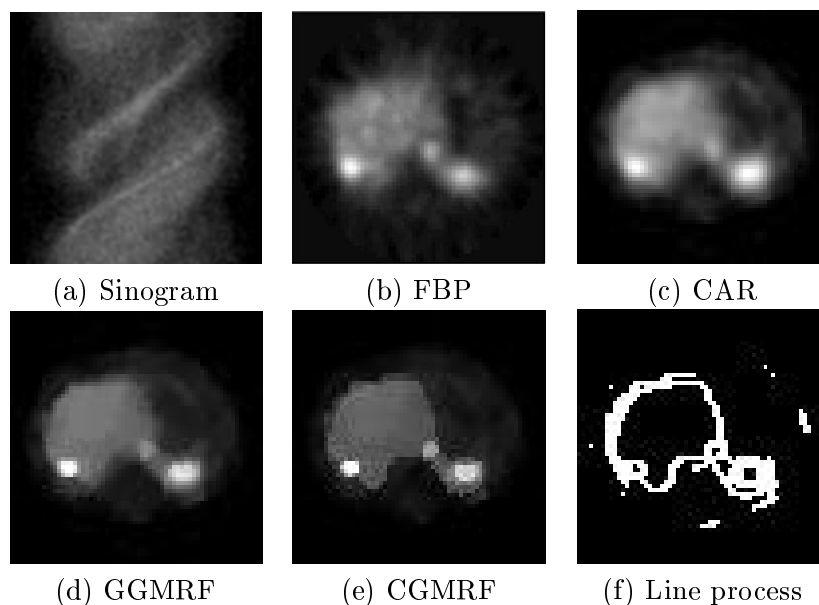


Figure 3: Results with a real image.

References

- [1] A. C. Kak and M. Slaney. *Principles of Computerized Tomographic Imaging*. IEEE Press, 1988.
- [2] S. Geman and S. Geman. Stochastic relaxation, gibbs distributions, and the bayesian restoration of images. *IEEE Trans. Pattern Analysis and Machine Intelligence*, 6:721–741, 1984.
- [3] F. C. Jeng and J. W. Woods. Simulated annealing in compound gaussian random fields. *IEEE Trans. Information Theory*, 36:94–107, 1988.
- [4] B. Ripley. *Spatial Statistic*. Wiley, New York, 1981.
- [5] R. Molina, A. K. Katsaggelos, J. Mateos, and J. Abad. Restoration of severely blurred high range images using compound models. In *ICIP-96*, 2, pages 469–472, 1996.
- [6] C. Bouman and K. Sauer. A generalized gaussian image model for edge-preserving map estimation. *IEEE Trans. Image Processing*, 2(3):296–310, 1993.
- [7] A. López, R. Molina, and A. K. Katsaggelos. Hyperparameter estimation for emission computed tomography data. In *ICIP-99*, 2, pages 667–680, 1999.